



Parameter Sensitivity Analysis of Pit Initiation at Single Sulfide Inclusions in Stainless Steel

M. Kamrunnahar, R. D. Braatz, and R. C. Alkire*^z

*Department of Chemical and Biomolecular Engineering and National Computational Science Alliance,
University of Illinois, Urbana, Illinois 61801, USA*

Sensitivity analysis methods were used in conjunction with a mathematical model for corrosion pit initiation in the vicinity of MnS inclusions in stainless steel to investigate the relationship between physicochemical parameters and the potential and concentration distributions. The finite difference method with central differences was used to calculate sensitivities. The mathematical model of pit initiation included 20 species plus the potential and 13 physicochemical parameters including rate constants for chemical and electrochemical surface reactions and equilibrium constants for homogeneous reactions. It was found that the potential and concentration profiles are most sensitive to the Tafel slope of the rate of electrochemical dissolution of sulfur-containing inclusions and least sensitive to changes in the equilibrium coefficients of the homogeneous reactions. The rate constant for the electrochemical reaction for dissolution of sulfide inclusions was also found to be significant. The procedure provides a first step toward selecting the most important parameters, designing critical experiments, and selecting the hypothesis that best fits experimental data.

© 2004 The Electrochemical Society. [DOI: 10.1149/1.1638384] All rights reserved.

Manuscript submitted February 26, 2003; revised manuscript received August 26, 2003. Available electronically January 9, 2004.

Pitting corrosion of stainless steel (SS) is a localized phenomenon that may initiate at various types of surface sites including sulfide inclusions. Interest in pitting corrosion is high because it is often a first step leading to crevice corrosion, corrosion fatigue, stress-corrosion cracking, and failure of coatings. The various mechanisms by which initiation occurs, a subject of longstanding interest, have increasingly been investigated with the aid of mathematical models. While there are various modeling approaches, we focus here on an approach where the underlying physical phenomena associated with the mechanisms are expressed by continuum equations for reaction, transport, and equilibration among species. Although numerical simulation of complex corrosion systems can provide useful insight, there is also the need for additional numerical methods. In this work we focus on the assessment of uncertainty. For example, the validation of models by comparison with experimental data requires specification of the hypothesis of corrosion mechanism (of which the literature provides multiple reasonable choices) as well as values for the system parameters (some of which may be difficult or impossible to measure directly). Various kinds of uncertainty therefore arise. The motivation for the present work is to apply numerical analysis tools to identify the most sensitive parameters associated with one particular hypothesis of mechanism. Such tools may find use in addressing questions such as: What properties of a system are responsible for its observed behavior? What is the most promising experiment to refute or confirm a model? Which of several hypotheses best agrees with experimental data from heterogeneous sources?

The role of sulfide inclusions has been widely investigated. Sulfide inclusions play an important role in the initiation of pitting corrosion. Various researchers have studied initiation of pitting corrosion with a range of experimental techniques to clarify various events during early stages of sulfide inclusion dissolution, (*e.g.*, Ref. 1-3) and pit growth. Sulfur-containing species have been detected during dissolution of sulfide inclusions,⁴⁻⁸ and pH measurements have been taken at various locations during sulfide dissolution.⁹ The influence of applied mechanical stress on pit initiation has been investigated.¹⁰ More recently, an electrochemical microcell was used to obtain electrochemical data and chemical composition at the vicinity of the sulfide inclusions.^{11,12}

In the present work we consider in detail a mathematical model of one particular mechanism developed to simulate pit initiation at a single MnS inclusion in SS within an electrochemical microcell.¹³ The model examined the hypotheses that pit initiation occurs by

depassivation of SS as a result of accumulation of thiosulfate ions above a critical concentration in the presence of chloride, and that the rate of inclusion dissolution was catalyzed by chloride. The model was used to predict the variation of potential in time and distance during the pit initiation and also to predict the dependence of pitting potential on the chloride concentration for a single inclusion. The emphasis in the present work is to apply numerical procedures for assessment of parameter sensitivity and to demonstrate their use with one hypothesis of mechanism.

In this work, the system of coupled nonlinear equations reported previously¹³ was solved numerically using a finite difference method whose solution at each time step involved the solution of 120,771 algebraic equations for a chloride-containing system. Parameters in the simulation model included diffusion coefficients of 20 different species, chemical/electrochemical rate constants, and equilibrium constants. The numerical values of many of these parameters reported in literature vary widely. However, it is well known that the dynamic behavior of a complex chemical transport system is often specified by the values of only a subset of all the parameters¹⁴ and that variations in the other parameters have a small effect. As a simple example of this, consider five first-order reactions in series where the rate constants for the last four reactions are a factor of ten larger than the rate constant for the first reaction. The concentration *vs.* time plots for all chemical compounds in the system are very sensitive to changes in the rate constant for the slowest reaction but are relatively insensitive to variations in the rate constants of the fast reactions. A similar effect occurs in complex reaction networks, which have many reactions in parallel, in series, and intimately coupled. In such systems, experimental effort is reduced by focusing only on determining the values for the most critical parameters.

Parameter sensitivity analysis is used to determine which of the parameters are the most significant by determining the effect of perturbing the parameters on the process outputs.¹⁴ Such analysis aids in selecting those parameters to be estimated for further analysis using simulation and/or experimental data and in designing future experiments. Parameter sensitivity analysis is a well-developed area¹⁵ and has been applied in many engineering applications in which mathematical models are used. While many applications of mathematical modeling to corrosion have been reported,¹⁶⁻²³ to our knowledge parameter sensitivity analysis has yet to be used to analyze mathematical models. In this study, parameter sensitivity analysis was applied to the pit initiation model developed by Webb and Alkire.¹³ The perturbation effects of thirteen parameters on 21 output variables were investigated. The output variables considered were the potential and concentrations of 20 species at the bottom of

* Electrochemical Society Fellow.

^z E-mail: r-alkire@uiuc.edu

a microrevice which is believed to be the most probable location for pit initiation.¹³ A brief summary of the mathematical model for pit initiation in SS is given in the Appendix.

Parameter Sensitivity Analysis

A formal definition of parameter sensitivity can be given as “the effect of parameter changes on the dynamics of a system, that is, the time response, the state, the transfer function, or any other quantity characterizing the system dynamics.”¹⁵ In parameter sensitivity analysis, each parameter in the model is perturbed to determine how sensitive the model outputs are to the changes in the parameter. A sensitivity is defined as the partial derivative of an output variable with respect to a parameter where the “nominal” parameters are the base case parameters for which the model is initially developed. For example, consider the mathematical model of a system

$$\mathbf{y} = f(x, t, \beta) \quad [1]$$

where \mathbf{y} is a vector of output or dependent variables, x and t are independent variables, β is a parameter vector, and f is a dynamic operator representing the output of a system of coupled partial differential equations. Then the first derivative of \mathbf{y}_i with respect to β_j is the sensitivity

$$s_{ij} = \frac{\partial \mathbf{y}_i}{\partial \beta_j} \quad [2]$$

and the matrix

$$S = \begin{bmatrix} s_{11} & s_{12} & \cdots & s_{1p} \\ s_{21} & s_{22} & \cdots & s_{2p} \\ \vdots & \vdots & \ddots & \vdots \\ s_{n1} & s_{n2} & \cdots & s_{np} \end{bmatrix} \quad [3]$$

is called the sensitivity matrix, where n is the number of observed outputs and p is the number of parameters. Another quantity that is commonly used is the normalized sensitivity

$$\hat{s}_{ij} = \frac{\beta_j}{\mathbf{y}_i} \cdot \frac{\partial \mathbf{y}_i}{\partial \beta_j} \quad [4]$$

Thus the normalized sensitivity matrix is

$$\hat{S} = \begin{bmatrix} \hat{s}_{11} & \hat{s}_{12} & \cdots & \hat{s}_{1p} \\ \hat{s}_{21} & \hat{s}_{22} & \cdots & \hat{s}_{2p} \\ \vdots & \vdots & \ddots & \vdots \\ \hat{s}_{n1} & \hat{s}_{n2} & \cdots & \hat{s}_{np} \end{bmatrix} \quad [5]$$

The advantage of the normalized sensitivity matrix is that its elements are not functions of the units of the parameters.

There are many methods for the determination of the partial derivatives including the direct differentiation method, the Green's function method, and the finite difference method.¹⁴ In the direct differentiation method, the sensitivities are obtained by differentiating the differential equations for the mathematical model with respect to each parameter. This introduces $n \times p$ more differential equations to be solved in addition to the original n differential equations, which is quite computationally expensive. The computational cost can be reduced by careful implementation of the numerical algorithms used to compute the sensitivities.²⁴ In the Green's function method, $n \times n$ differential equations plus n integrals are solved. This method is more computationally efficient than the direct differentiation method when the number of parameters is much larger than the number of outputs. Another method known as the adjoint method also has computational advantages for such problems.²⁵

The finite difference method typically uses a forward or a central difference approximation of the partial derivatives

$$s_{ij} = \frac{\partial \mathbf{y}_i}{\partial \beta_j} \approx \frac{\Delta \mathbf{y}_i}{\Delta \beta_j} \approx \frac{\mathbf{y}_i(\beta_j + \Delta \beta_j) - \mathbf{y}_i(\beta_j - \Delta \beta_j)}{2\Delta \beta_j} \quad [6]$$

To estimate the sensitivities using the central difference approximation, n differential equations are solved twice (one for negative perturbation and the other for positive perturbation) for each parameter. Each perturbation should be selected small enough that the effect of the higher order nonlinear terms in the finite difference approximation is negligible and large enough that the calculations are not significantly influenced by the simulation tolerance.

The particular method to be used for sensitivity calculations depends on the application. The finite difference method is the easiest to implement for systems of coupled nonlinear partial differential equations and was used here.

Parameter Sensitivity Analysis of the Pit Initiation Model

The continuum model for pit initiation described in the Appendix has 21 output variables that include the solution potential and the concentrations of 20 species at different locations in the simulation domain. The physicochemical parameters investigated using sensitivity analysis were the reaction rate constants (both chemical and electrochemical), the equilibrium constants, and the Tafel slope of the rate of the electrochemical dissolution (m) (see Table I).

The effects of thirteen parameters were determined, which required $2 \times (\text{no. of perturbed parameters}) + 1 = 27$ sets of perturbed parameters. The code for the numerical solution of the model was written with an object-oriented programming approach which composed the model from objects that were placed outside of the region of code that solves the model equations. In this manner, the particular choice of species, reactions, system parameters, solution compositions, and geometry can be altered without additional code modifications. Twenty-seven jobs for the 27 parameter sets were created to solve the numerical problem without changing the source code.

The accuracy of the finite difference estimates is a function the magnitude of the perturbation, $\Delta \beta$, which should be small enough that the effect of the higher order terms in the finite difference approximation is negligible, yet large enough that the estimate is insensitive to the simulation tolerance. For a complex reaction model the effect of the higher order terms is not known *a priori*, so it is standard practice to compute the estimates for a range of values for $\Delta \beta$.¹⁴ In this paper, simulations were performed for 5, 10, 20, and 30% perturbations in each parameter to see the effects on the estimates. Also, performing several perturbation magnitudes is useful for model understanding in its own right, as it allows a determination of which parameters have a strong nonlinear effect on the process outputs.

The simulations for multiple parameter sets were carried out in “super batch” mode on an SGI Origin 2000 at the National Center for Supercomputing Applications (NCSA) at the University of Illinois. Parallel computational technique was used to solve the numerical problem because there were 27 sets of parameters, each of which involved many equations to be solved simultaneously and required substantial amount of computational time and resources. The use of PETSc (Portable, Extensible Toolkit for Scientific Computation),²⁶ a set of numerical solvers and data structures, allowed efficient parallelization of the code that resulted in a significant decrease in computational time. To calculate the sensitivities, outputs from the PETSc solver required some format changes. Outputs of the simulation code were postprocessed to obtain the simulation output data in the proper format for further analysis. The sensitivities were then calculated using the finite difference expression in Eq. 6.

Results and Discussion

According to the hypothesis and model under consideration here,¹³ pit initiation occurs at the bottom of the microrevice adja-

Table I. Heterogeneous and homogeneous chemical reactions with kinetic and equilibrium parameters.

Parameter for chemical reactions	
Reactions	k (cm ² /s)
MnS + H ⁺ ↔ Mn ²⁺ + HS ⁻	0.74
Rate: $r_c = k[H^+]$	
Parameters for electrochemical reactions	
Reactions	i_{MnS}^0 (A/cm ²) m (mV ⁻¹)
2MnS + 3H ₂ O ↔ 2Mn ²⁺ + S ₂ O ₃ ²⁻ + 6H ⁺ + 8e ⁻	0.0006 0.02574
Rate: $i_{MnS} = i_{MnS}^0 \exp[m(E_{app} - E_{MnS} - \Phi)]$	
Parameters for homogeneous equilibrium reactions	
Reactions	Equilibrium Constant, K
Cr ³⁺ + H ₂ O ↔ CrOH ²⁺ + H ⁺	1.0 × 10 ⁻⁴
Cr ³⁺ + 2H ₂ O ↔ Cr(OH) ₂ ⁺ + 2H ⁺	2.0 × 10 ⁻¹⁰
Mn ²⁺ + Cl ⁻ ↔ MnCl ⁺	4.07
Mn ²⁺ + 2Cl ⁻ ↔ MnCl ₂	1.09
Fe ²⁺ + Cl ⁻ ↔ FeCl ⁺	7.94
Fe ²⁺ + 2Cl ⁻ ↔ FeCl ₂	25.1
Cr ³⁺ + Cl ⁻ ↔ CrCl ²⁺	5.01
Cr ³⁺ + 2Cl ⁻ ↔ CrCl ₂ ⁺	50.1
S ₂ O ₃ ²⁻ + H ⁺ ↔ HS ₂ O ₃ ⁻	50.0
H ₂ S ↔ HS ⁻ + H ⁺	1.0 × 10 ⁻⁷

cent to a sulfide inclusion. The output variables of the model were therefore obtained at this location. Quantitative results are presented in terms of normalized sensitivity coefficients, which are easier to interpret because they are not a function of the units of the parameters. The sensitivities in Eq. 2 are a function of the units or scaling of the parameters, which can be misleading if not interpreted carefully.

The base case calculations for the chloride chemistry were carried out for a 100 μm diam microcell with a 20 μm diam MnS

inclusion at 150 mV overpotential ($E_{app} - E_{MnS}$), pH 6, and 1.0 M NaCl. The base case parameters selected for the sensitivity analysis are shown in Table I. In addition, the variation of overpotential from 150 to 300 mV was carried out.

Effect of electrochemical rate constant.—The results of perturbing the electrochemical rate constant i_{MnS}^0 from the base case value at 150 mV overpotential for the species involved in Eq. A-1 are shown in Fig. 1 and in Table II. The potential is significantly sensitive to perturbations in the electrochemical rate constant with a normalized sensitivity coefficient of 0.85. The pH and chromium ion concentrations are also significantly affected (sensitivity coefficients -0.1 and 0.035, respectively). The significant effects may be because the electrochemical reaction directly affects the hydrogen ion and Mn²⁺ concentrations, which affect the chromium ion concentrations (see Table I). Increasing i_{MnS}^0 produces more hydrogen ions (see Eq. A-1), which decreases the pH (as seen in Fig. 1). The chromium ion concentration depends nonlinearly on changes in the electrochemical rate constant larger than ±20%, whereas the effect on the other outputs is linear for the whole range of perturbations. The sensitivity estimates in Table II are consistent with a small deviation for the chloride concentration for perturbations of 5% and for the chromium ion concentration for perturbations larger than 10%.

Effect of Tafel slope of the electrochemical dissolution rate.—Changes in the Tafel slope of the electrochemical dissolution rate m on the outputs are reported in Fig. 2 and Table II. The effect on the potential is very large (sensitivity coefficients 3.31-4.75), and this effect is nonlinear except for the smallest perturbations. The effect on the pH is significant, but linear. The effect on the chromium ion concentration is nonlinear and much smaller for an increase in the slope of the electrochemical dissolution rate than a decrease. The nonlinear effect of this parameter on the potential and chromium ion concentration is due to the exponential nature of the electrochemical rate in Eq. A-2. The effect of m on the chloride ion concentration is not significant (sensitivity coefficient 0.0025). The possible reason for the insignificant effect is that the base case over-

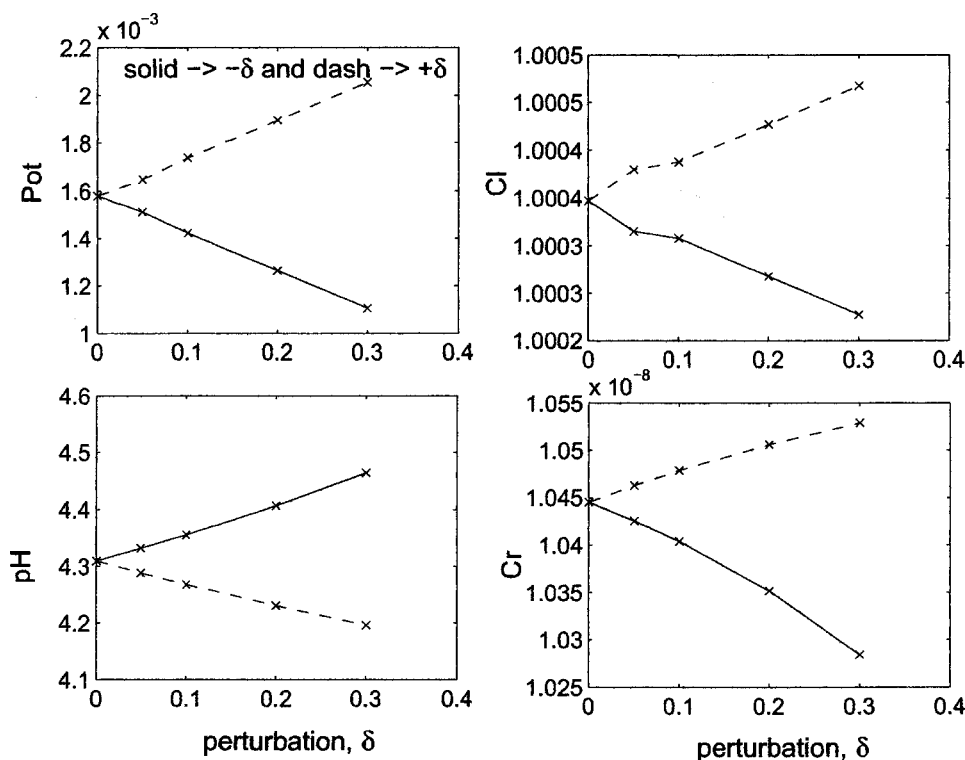


Figure 1. Dimensionless potential and concentration profiles for perturbations in the electrochemical reaction rate, i_{MnS}^0 .

Table II. Normalized sensitivities part 1.^a

Out, parameter	$I_{MnS}^0 \times 10^2$	$m \times 10^2$	$k \times 10^3$	$K_{CrOH} \times 10^4$	$K_{Cr(OH)_2} \times 10^4$
	5%				
Pot	85.4	331.74	-6.63	0.0663	0.0294
Cl	0.065	0.25	-0.019	0	0
pH	-10.1	-38.8	99.6	-0.0024	0.0053
Cr	3.52	13.7	-37.2	-347	-18.2
	10%				
Pot	99.8	361	-6.66	-0.011	-0.0736
Cl	0.0399	0.216	-0.0197	0	0
pH	-10.1	-38.8	99.8	-0.0011	0.0003
Cr	3.58	13.9	-37.0	-348	-14.0
	20%				
Pot	99.83	424	-6.82	0.0368	0.0055
Cl	0.0399	0.169	-0.02	0	0
pH	-10.2	-38.8	101	-0.0005	0.0011
Cr	3.70	15.0	-37.1	-347	-13.5
	30%				
Pot	99.8	475	-7.13	-0.0123	-0.0282
Cl	0.0399	0.19	-0.021	0	0
pH	-10.4	-38.8	103	-0.00047	-0.00052
Cr	3.91	16.9	-37.0	-348	-14.1

^a The largest values are boldface.

potential (150 mV) was not close to the pitting potential. Because of the significant effect of m on most of the outputs, this parameter requires special attention for further analysis, parameter estimation, and experimental design.

Effect of chemical rate constant.—The output variables resulting from changes in the chemical reaction rate constant k for MnS dissolution in Eq. A-3 are reported in Fig. 3 and the sensitivities are reported in Table II. The pH and chromium ion concentration were somewhat affected by perturbations in the chemical rate constant (sensitivity coefficients are 0.099 and -0.037 , respectively), whereas the changes in the potential and chloride ion concentration are insignificant (sensitivity coefficients are -0.0066 and -0.000019 , respectively). The significant effects on pH and chro-

mium ion concentration could be suspected from inspection of the heterogeneous and homogeneous chemical reaction network. An increase in the rate for the chemical reaction in Eq. A-3 directly depletes hydrogen ion, which results in a higher pH. An increase in the chemical rate constant k produces more Mn^{2+} ion, which can react with water to produce another hydrogen ion (see Table I). The effects of producing and depleting H^+ ion are not balanced, which directly affects the species concentrations in the homogeneous chemical reactions that include both hydrogen and chromium ions. As shown in Fig. 3, the output variables are more or less linear to changes in the chemical rate constant k , with the magnitude of the effect of positive perturbations on pH being slightly smaller than for

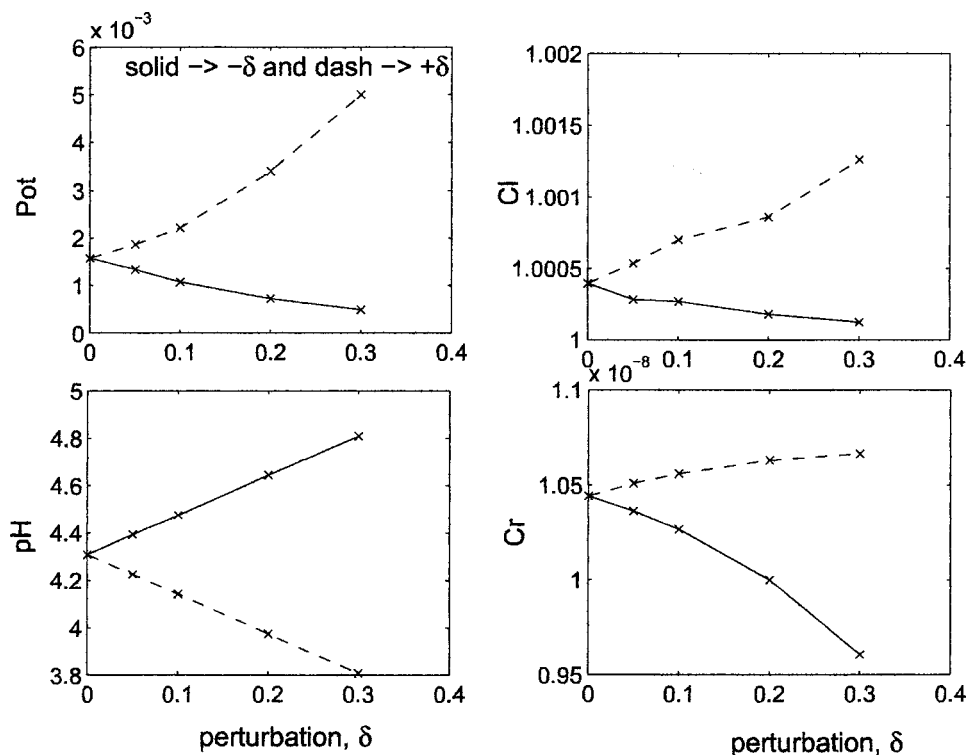


Figure 2. Dimensionless potential and concentration profiles for the perturbation in slope of the electrochemical dissolution, m .

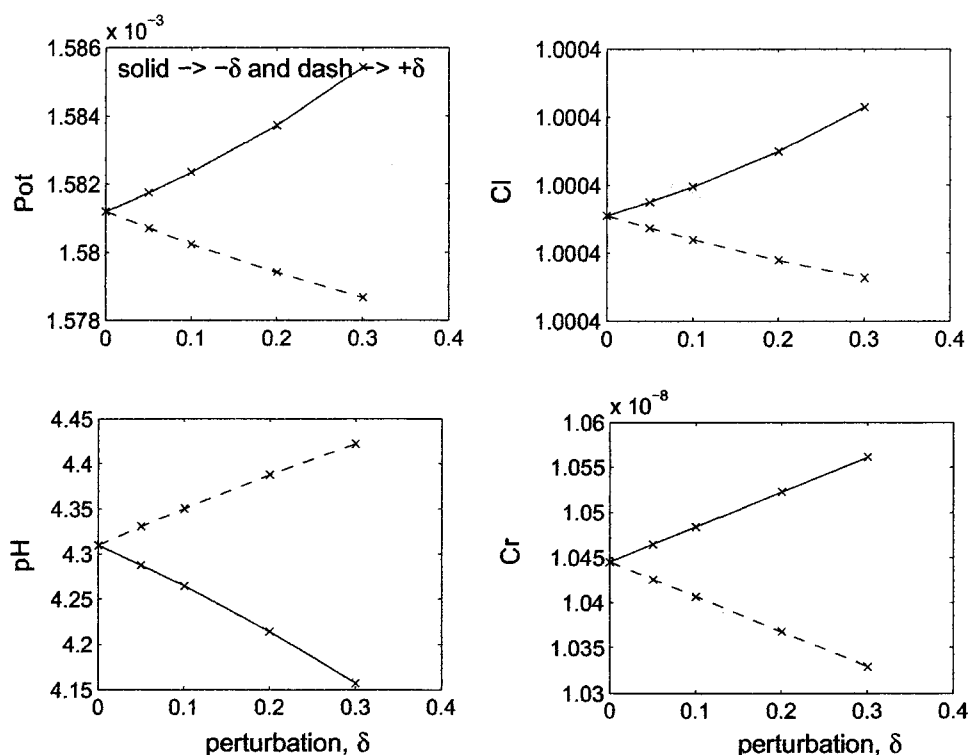


Figure 3. Dimensionless potential and concentration profiles for perturbations in the chemical reaction rate, k .

negative perturbations. As shown in Table II, the estimates of the sensitivities are consistent for a wide range in perturbations in the chemical rate constant k .

Effect of equilibrium constants.—The effects of perturbing the equilibrium constants $K_{\text{Cr}(\text{OH})}$ and $K_{\text{Cr}(\text{OH})_2}$ are presented in Table II. These two parameters had negligible effect on all the outputs except that $K_{\text{Cr}(\text{OH})}$ affected the chromium ion concentration in a linear manner. Except for the effect of $K_{\text{Cr}(\text{OH})}$ on the chromium ion concentration, which had consistent estimates for all perturbations, the sensitivities associated with these two equilibrium constants are very close to zero. This suggests that a simpler chemical reaction network may be sufficient in modeling pit initiation at the operating conditions used in the current model. However, at different operating conditions the equilibrium constants may be more significant.

Values of equilibrium constants for chromium hydrolysis reported in the literature vary widely, indicating these parameters are not known accurately. Because the sensitivity results indicate that

uncertainties in the value of these parameters have a negligible influence on most model outputs (especially for $K_{\text{Cr}(\text{OH})_2}$), there is not a strong motivation for doing *ab initio* thermodynamic calculations or focused experiments to determine the value of these parameters more accurately at the current operating conditions.

Quantitative results for perturbing the equilibrium constants for the other homogeneous reactions are reported in Table III. Most of the parameters have a small effect on the outputs, the exceptions being K_{MnCl_2} and K_{CrCl_2} , which affect the potential and chromium ion concentrations, respectively. These results were somewhat unexpected, because they indicate that accurate values of most of the equilibrium constants for the homogeneous reactions are not needed to model pit initiation. Perhaps the values for the constants may play a more important role for different operating conditions.

Effect of applied overpotential.—The effect of variation in applied overpotential ($E_{\text{appl}} - E_{\text{MnS}}$) on the parameter sensitivities was

Table III. Normalized sensitivities part 2.^a

Out, parameter	$K_{\text{MnCl}} \times 10^4$	$K_{\text{MnCl}_2} \times 10^3$	$K_{\text{FeCl}} \times 10^5$	$K_{\text{FeCl}_2} \times 10^5$	$K_{\text{CrCl}} \times 10^5$	$K_{\text{CrCl}_2} \times 10^3$	$K_{\text{HS}_2\text{O}_3} \times 10^5$	$K_{\text{HS}} \times 10^5$
	10%							
Pot	67.0	-118	14.0	-18.1	1.47	-0.0085	46.7	-111.0
Cl	0.220	-0.39	-0.0596	0.0596	0.00	0.00	0.0596	-0.179
pH	0.0067	-0.0125	-0.00081	-0.00755	-0.0096	0.0002	0.761	-2.72
Cr	-1.16	0.904	0.553	-8.46	-8520	-858	2.38	-0.638
	20%							
Pot	67.9	-119	13.8	-18.4	0.847	-0.0166	47.3	-111.0
Cl	0.220	-0.391	0.0596	-0.0596	0.00	0.00	0.089	-0.179
pH	0.0085	-0.0127	-0.0032	-0.00325	-0.0021	0.000187	0.776	-2.73
Cr	-0.234	0.925	-8.48	3.51	-8532	-878	-1.21	-3.53
	30%							
Pot	69.4	-119	13.5	-19.0	0.712	-0.0199	47.7	-111.0
Cl	0.224	-0.391	0.0397	-0.0596	0.00	0.00	0.0794	-0.199
pH	0.0071	-0.0127	0.00076	-0.00189	-0.0011	0.000069	0.76	-2.72
Cr	-0.710	0.838	0.652	0.595	-8530	-912	-2.11	3.34

^a The largest values are in boldface.

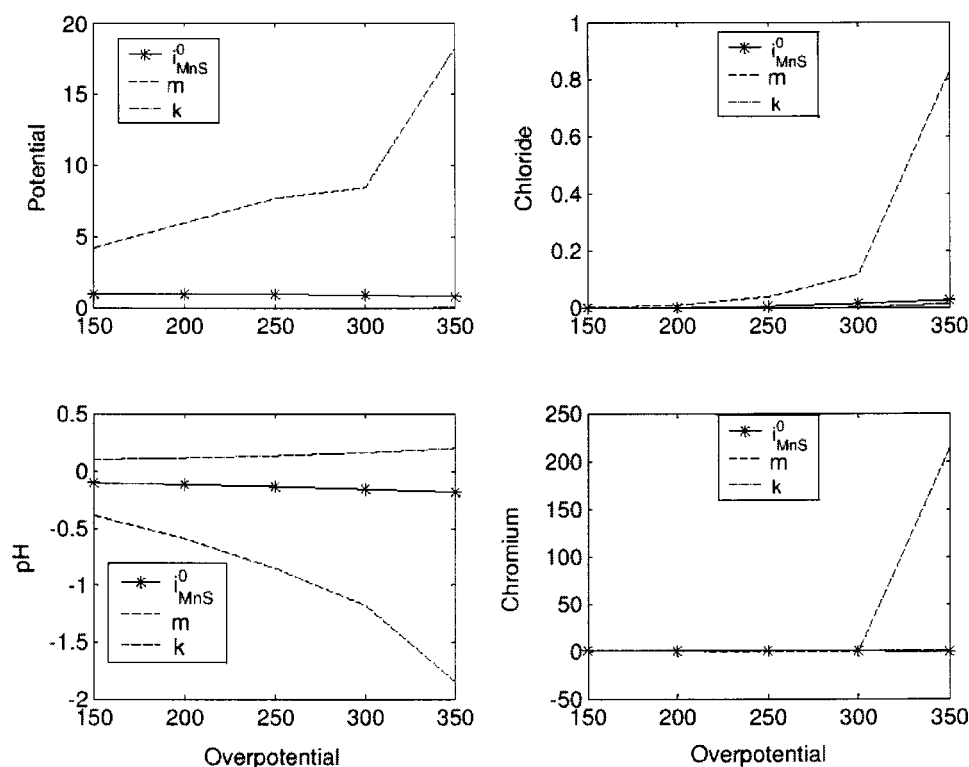


Figure 4. Effect of overpotential on the normalized sensitivities of the electrochemical reaction rate i_{MnS}^0 , Tafel slope m of the electrochemical dissolution, and chemical reaction rate k for a perturbation of 20%.

investigated over the range 150–300 mV. The sensitivities of the electrochemical rate i_{MnS}^0 , the Tafel slope m of the electrochemical dissolution, and the chemical rate constant k are shown in Fig. 4 for a perturbation of 20%. However, for normalized sensitivities, varying the size of perturbation did not change the sensitivities significantly. The sensitivities of other parameters did not show significant change with the variation in the overpotential. The largest effect of overpotential was on the sensitivities of the Tafel slope (m) for all output variables. We interpret the dependence of the sensitivity of m on overpotential to indicate that the importance of the electrochemical reaction becomes significant as overpotential ramps up, and certain aspects of the chemistry therefore turn on as the overpotential is increased.

Conclusions

Parameter sensitivity analysis was applied to a pit initiation model that examines the hypotheses that pit initiation occurs by depassivation of SS as a result of accumulation of thiosulfate ions above a critical concentration in the presence of chloride, and that the rate of inclusion dissolution was catalyzed by chloride. A finite difference method was used to calculate the normalized sensitivity coefficients for thirteen physicochemical parameters (shown in Table I) used in the mathematical model. The base case calculations were performed under steady-state conditions at the chemical environment: a single shallow sulfide inclusion (20 μm diam) with a microcrevice, positioned at the center of a 100 μm diam microcapillary containing 1.0 M NaCl at pH 6, and polarized to an overpotential ($E_{\text{appl}} - E_{\text{MnS}}$) of 150 mV.

Among the thirteen parameters investigated, the most significant was m , the Tafel slope of the electrochemical rate of MnS dissolution. The m parameter has a nonlinear effect on the output variables (see Fig. 2 and Table II) and the large magnitude of the effect indicates that it is important to estimate this parameter accurately.

The electrochemical rate constant for MnS dissolution has a significant effect on the potential (see Fig. 1 and Table II), some effect on the pH, and a small effect on the chromium ion concentration. This parameter should be included in future parameter estimation studies. Perturbing the chemical reaction rate k has some effect on

the pH and chromium ion concentration (see Fig. 3 and Table II). Only a few outputs were affected by variation of the equilibrium constants $K_{\text{Cr(OH)}}$, K_{MnCl_2} , and K_{CrCl_2} . All the outputs were insensitive to variations in the other equilibrium constants. The sensitivities of the m parameter were significantly affected by the variation in the applied overpotential (see Fig. 4) and needs to be investigated further.

The sensitivity analysis identified the important parameters such as m , which can help in the search for inhibitors of corrosion initiated at pits. As noted by Suter *et al.*,¹⁰ the slope of the polarization curve during MnS dissolution depends on the onset potential of the MnS dissolution. The more positive the onset potential, the steeper the increase of the dissolution peak, which results in an increasingly acidic environment that encourages pit dissolution.

The parameter sensitivity analysis indicates that one way to gain confidence in the predictive ability of the model would be to obtain direct experimental measurements of the concentrations of the species in Eq. A-1 and A-3 at single inclusions. These data could be incorporated in a direct parameter estimation algorithm to reduce the uncertainty in the values for the chemical and electrochemical kinetic rate parameters. Although not all of the species concentration in these equations can be measured in practice, the more that are measured, the better the parameters could be estimated. An alternative approach would be to apply maximum likelihood parameter estimation^{27,28} to all of the experimental data collected for single pit inclusions, where only the most important parameters identified in this study are included in the estimation procedure.

The results identified the physicochemical parameters that are the most sensitive in the chemistry studied by Webb and Alkire¹³ for the set of base case parameters. The object-oriented code written for the solution of the mathematical model allows its use to explore different chemistries and mechanisms for the pit initiation process without additional code modifications. Performing parameter sensitivity analysis on other hypothesized chemical mechanisms and comparing the results to experiments can be used to assess which hypothesis of mechanism best describes pit initiation.

Acknowledgments

Funding for this project was provided by the National Computational Science Alliance and the National Science Foundation under grant ACI 96-19019. Computational resources at the National Center for Supercomputing Applications (NCSA) at the University of Illinois were used to perform the analysis. Discussions with T. Suter at the Swiss Federal Institute of Technology were very helpful. Discussions and computational help from J. Gray and J. Alameda are acknowledged.

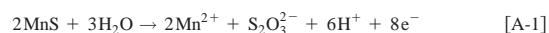
The University of Illinois assisted in meeting the publication costs of this article.

Appendix

Model for Pit Initiation at Single Sulfide Inclusions

The mathematical model of Webb and Alkire¹³ was developed for simulating the pitting potential based on the local chemical environment produced by dissolution of a sulfide inclusion on stainless steel. The key hypotheses were that pit initiation occurs by depassivation of SS as a result of accumulation of thiosulfate ions above a critical concentration in the presence of chloride, and that the rate of inclusion dissolution was catalyzed by chloride. The 2D circular cylindrical domain used for the simulation is shown in Fig. A-1. The simulation region ABCDEFGH corresponded closely to the experimental arrangement.¹¹ A MnS inclusion was assumed to be positioned at the center of a microcell and a microcrevice was assumed at the edge of the inclusion. Surface CD of the microcrevice consisted of MnS and the remaining surfaces consisted of SS. BCDEFG was considered the working electrode and the AH line was far enough away that the solution concentrations can be assumed to be at the bulk concentration.

At high overpotential the dissolution of MnS was assumed to take place by the following electrochemical reaction to form thiosulfate



The rate of the electrochemical reaction is written as

$$i_{\text{MnS}} = i_{\text{MnS}}^0 \exp[m(E_{\text{appl}} - E_{\text{MnS}} - \Phi)] \quad [\text{A-2}]$$

Inclusion dissolution due to the chemical reaction



was also assumed to occur with the reaction rate

$$r_c = kc_{\text{H}^+} \quad [\text{A-4}]$$

where c_{H^+} is the hydrogen ion concentration.

Two metal dissolution reactions were considered for the dissolution of SS. The SS was assumed to dissolve in proportion to the ratio of the metal elements in the steel. Because the hydrolysis and equilibrium constants of Fe^{2+} and Ni^{2+} are similar, the chemistry of Ni^{2+} could be combined with the dissolution and homogeneous reactions of Fe^{2+}



The fraction, f_i , of the current corresponding to the dissolution of each metal ion was given by

$$f_i = \frac{z_i M_i}{\sum_j z_j M_j} \quad [\text{A-7}]$$

The SS flux on the passive surface was set at $1 \mu\text{A cm}^{-2}$, a value obtained from experimental measurements.¹¹

Twelve reversible homogeneous reactions assumed to occur during the pit initiation process were described in Table I of Ref. 13 for the chloride-containing chemistry. The species involved in the reactions are listed in Table I.

A material balance equation for each species is

$$\frac{\partial c_i}{\partial t} = -\nabla \cdot N_i + R_i \quad [\text{A-8}]$$

where the flux is

$$N_i = -z_i u_i F c_i \nabla \Phi - D_i \nabla c_i \quad [\text{A-9}]$$

The mobility was estimated by the Nernst-Einstein equation

$$D_i = RTu_i \quad [\text{A-10}]$$

The equilibrium reactions satisfy

Bulk Concentrations

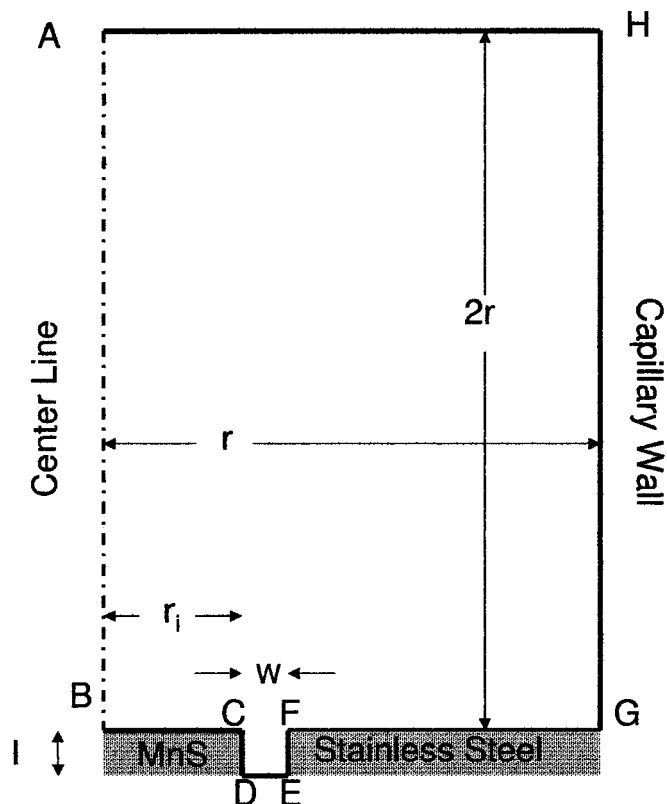


Figure A-1. Domain of single shallow MnS inclusion within microelectrochemical cell. Reproduced with permission from The Electrochemical Society.¹³

$$\frac{c_i^\alpha c_j^\beta}{c_k^\delta} = K_{\text{eq}} \quad [\text{A-11}]$$

The solution was assumed to be electrically neutral

$$\sum_k z_k c_k = 0 \quad [\text{A-12}]$$

and the current density is related to the flux by

$$i = F \sum_i z_i N_i \quad [\text{A-13}]$$

It was assumed that the passive steel surface EFG is in the same passivation level up to the end of the pit initiation.

The boundary conditions considered for the solution of the numerical problem are: (i) at the line AH, the species concentrations were assumed to equal the bulk values and the potential was set at a reference value of zero, (ii) the electroneutrality condition was satisfied and normal fluxes were zero at the surface GH, (iii) for nonreactive species, the fluxes were zero at the surface BG, (iv) electroneutrality was assumed to hold at the surface of the inclusion (BC and CD), and (v) at the line of symmetry, AB, concentration gradients and the potential gradient were zero. Details on the boundary conditions can be found in Ref. 13.

The model was nondimensionalized and solved using the finite difference method described previously.¹³ The resulting nonlinear algebraic equations were solved using PETSc,²⁶ which is a set of numerical solvers and data structures developed for the parallel solution of systems of equations resulting from the discretization of partial differential equations. PETSc uses MPI (Message Passing Interface) for communications between processors.

List of Symbols

c_i	concentration of species i , M
E	electrochemical potential, mV vs. SCE
D_i	diffusion coefficient of species i , $\text{cm}^2 \text{s}^{-1}$
E_{appl}	applied potential, mV vs. SCE
E_{MnS}	onset potential of MnS dissolution, mV vs. SCE

F Faraday's constant, C equiv⁻¹
 i_{SS} stainless steel current density, A cm⁻²
 i_{MnS} MnS current density, A cm⁻²
 k reaction rate constant of MnS chemical dissolution, cm s⁻¹
 K_i equilibrium constant of species i for homogeneous reaction, M or M²
 l depth of the microcrevice, cm
 m Tafel slope of the electrochemical MnS dissolution reaction, mV⁻¹
 n number of electrons in reaction, equiv mol⁻¹
 N_i flux of species i, mol cm⁻² s⁻¹
 r radius of the microelectrochemical cell, cm
 r_i radius of MnS inclusion, cm
 r_c rate of chemical dissolution of MnS inclusion, mol cm⁻² s⁻¹
 R_i rate of homogeneous reaction i, mol cm⁻³ s⁻¹
 ν_i^k stoichiometry of species i in reaction k, dimensionless
 u_i electrochemical mobility of species i, cm² mol⁻¹ s⁻¹
 w width of the microcrevice, cm
 z_i ionic charge of species i

Greek

Φ solution phase potential, mV

References

- D. E. Williams, T. F. Mohiuddin, and Y. Y. Zhu, *J. Electrochem. Soc.*, **145**, 2664 (1998).
- J. E. Castle and R. Ke, *Corros. Sci.*, **30**, 409 (1990).
- M. A. Baker and J. E. Castle, *Corros. Sci.*, **34**, 667 (1993).
- G. Eklund, *J. Electrochem. Soc.*, **121**, 467 (1974).
- G. Wranglen, *Corros. Sci.*, **14**, 331 (1974).
- E. G. Webb, C. H. Paik, and R. C. Alkire, *Electrochem. Solid-State Lett.*, **3**, 416 (2000).
- C. S. Brossia and R. G. Kelly, in *Critical Factors of Localized Corrosion II*, P. M. Natishan, R. G. Kelly, G. S. Frankel, and R. C. Newman, Editors, PV 95-15, p. 201, The Electrochemical Society Proceedings Series, Pennington, NJ (1996).
- C. S. Brossia and R. G. Kelly, *Corros. Sci.*, **40**, 1851 (1998).
- J. O. Park and H. Bohni, *Electrochem. Solid-State Lett.*, **4**, B15 (2001).
- T. Suter, E. G. Webb, H. Bohni, and R. C. Alkire, *J. Electrochem. Soc.*, **148**, B174 (2001).
- E. G. Webb and R. C. Alkire, *J. Electrochem. Soc.*, **149**, B272 (2002).
- E. G. Webb and R. C. Alkire, *J. Electrochem. Soc.*, **149**, B280 (2002).
- E. G. Webb and R. C. Alkire, *J. Electrochem. Soc.*, **149**, B286 (2002).
- A. Varma, M. Morbidelli, and H. Wu, *Parameter Sensitivity in Chemical Systems*, Cambridge University Press, New York (1999).
- P. M. Frank, *Introduction to Systems Sensitivity*, Academic Press, New York (1978).
- J. R. Gavele, *J. Electrochem. Soc.*, **123**, 464 (1976).
- R. C. Alkire and S. E. Lott, *J. Electrochem. Soc.*, **136**, 3256 (1989).
- S. M. Sharland and P. W. Tasker, *Corros. Sci.*, **28**, 605 (1988).
- S. M. Sharland, *Corros. Sci.*, **28**, 621 (1988).
- J. C. Walton, *Corros. Sci.*, **30**, 915 (1990).
- S. M. Sharland, *Corros. Sci.*, **33**, 183 (1992).
- S. P. White, G. J. Weir, and N. J. Laycock, *Corros. Sci.*, **42**, 605 (2000).
- G. Englehardt, M. Urquidi-Macdonald, and D. D. Macdonald, *Corros. Sci.*, **39**, 419 (1997).
- W. F. Feehery, J. E. Tolsma, and P. I. Barton, *Appl. Numer. Math.*, **25**, 41 (1997).
- R. Serban and L. R. Petzold, *SIAM (Soc. Ind. Appl. Math.) J. Numer. Anal.*, **40**, 220 (2002).
- S. Balay, K. Buschelman, W. D. Gropp, D. Kaushik, L. C. McInnes, and B. F. Smith, PETSc home page, <http://www.mcs.anl.gov/petsc> (2001).
- J. V. Beck and K. J. Arnold, *Parameter Estimation in Engineering and Science*, John Wiley & Sons, New York (1977).
- R. Gunawan, D. L. Ma, M. Fujiwara, and R. D. Braatz, *Int. J. Mod. Phys. B*, **16**, 367 (2002).